PORT SAID ENGINEERING RESEARCH JOURNAL
Faculty of Engineering - Port Said University
Volume 28 No. 2 pp: 31 : 40

Evaluation of Geogrid-Aperture Size on the Behavior of Reinforced Fine-Sand Supporting a Square Footing

Essam Badrawi

Structural Engineering Department, Faculty of Engineering, Zagazig University, Zagazig, Egypt, email: e.f.b.attia@gmail.com,

DOI: 10.21608/PSERJ.2024.253865.1297

Received 13-12-2023,
Revised 20-1-2024,
Accepted 22-1-2024

ABSTRACT

Fine-sand soils cannot support the design loads due to their low load-bearing capacity. Soil reinforcement with geogrid-layers is a common technique to increase the low bearing capacity of fine-sand. Using the commercial finite element analysis package Abaqus (Ver. 2017), a three-dimensional numerical model is used to determine the effect of geogrid-aperture size on the square footing bearing capacity of geogrid-reinforced fine-sand. In the numerical analysis, the geogrid-aperture size ratio ranged from 1.0 to 4.0. These variations in the geogrid-aperture size ratio were used to estimate the effect of first geogrid-layer depth (u/B), geogrid-layer width (b/B), vertical spacing between geogrid-layers (h/B), and the geogrid-layers number (N) on the bearing capacity ratio (BCR) and the horizontal stress ratio (HSR), which were transferred to the fine-sand through geogrid-layers. The bearing capacity of a square footing on geogrid-reinforced fine-sand increases with inclusion of a geogrid-layer, provided it has the appropriate dimensions and numbers. The horizontal stresses transferred to the fine-sand through the geogrid-layers also increased. The results indicate that the interlocking between fine-sand and the geogrid-layers increases due to the reduced movement of fine-sand particles. For the variation of geogrid-aperture size ratio from 1.0 to 4.0, the maximum decrease rates of the (BCR), HSR-(Cross), and HSR-(Machine) values are 12.06%, 15.25%, and 18.22%, respectively. The optimal values of (u/B), (b/B), (h/B) and (N) are 0.3, 3.0, 0.15, and 3.0 for all values of geogrid-aperture size ratio. For the maximum (BCR) values of the square footing on fine-sand, using a biaxial geogrid-layer is considered more efficient than using a uniaxial geogrid-layer.

Keywords: Numerical analysis, square footing, Geogrid-Aperture Shape size, Fine-sand.

1. INTRODUCTION

The bearing capacity of fine-sand supporting a square footing is limited under vertical loads, and settlement and bearing capacity problems due to the underlying soil. One of the most common techniques to reduce soil settlement and increase low bearing capacity values is soil reinforcement with the geogrid-layer. The interlocking between geogrid-layer and soil particles minimizes the lateral movement of the soil particles; the confinement of the particles leads to an increase in soil bearing capacity and reduced soil settlement. The effectiveness of the interlocking between the geogrid-layer and the soil particles depends on the relationship between the geogrid-aperture size and the soil particle size [1]. Uniaxial and biaxial geogrid-layers are two typical types of geogrid successfully used in soil reinforcement techniques. Uniaxial geogrid-layer have tensile strength in one direction (Machine direction), while biaxial geogrid-layer have tensile strengths in two directions (Machine and Cross directions). In recent decades, several experimental and numerical models have been carried out to evaluate the bearing capacity of shallow foundations on sand or clay beds reinforced with single or multi-layer geogrid. Additionally, the load-settlement curves and the settlement reduction ratio were also evaluated. Shafi [2] studies the effect of a triaxial geogrid-layer on the bearing capacity of poorly-graded medium sand supporting a square footing. The optimal depth and width values of first geogrid-layer

are 0.45 times and 5.50 times the footing width, respectively. Prasad [3] presents an experimental study to investigate stress-settlement behavior for a square footing on two types of granular soil: (a) geogrid-reinforced sand layer and (b) geogrid-reinforced aggregate over sand layer. The optimal depth of geogrid-layer for the aggregate over the sand layer decreased to 0.30 times the footing width from 0.45 times the footing width for the sand layer only case. Ahmadi [4] describes an experimental pull-out test using five geogrid types with different aperture sizes and four soil types with different particle sizes. For each soil type, a large geogrid-aperture size reduces the friction force between soil and geogrid-layer, the optimal geogrid size depends on the soil particle size. In addition, the transverse ribs of the geogrid-layer were more sensitive than the longitudinal ribs to withstand applied loads. S. K. Das [5] investigated the pre-stressing effect of geogrid-layer on bearing capacity and settlement performance for the cases of unreinforced (UR), geogrid-reinforced (GR), and pre-stressed geogrid-reinforced (PGR) soil. The top soil layer consists of well-graded medium sand overlying the weak soil layer (SP-ML). The PGR soil can increase the bearing capacity of unreinforced sand by 500% and decrease settlement by 88%. Compared to geogrid-reinforced soil, pre-stressed geogrid-reinforced soil provides better performance when the square foundation is positioned at greater depths. Additionally, the placement of two adjacent-square footings increases the interference zone of pre-stressed geogrid-reinforced soil by 67% compared to unreinforced soil. Jianjun Fu [6] uses the coupled discrete element method (DEM) to simulate the pullout test and evaluate the effect of geogrid-aperture shapes, (square and triangular) on the ballast soil behavior. In the fully confined zone, the triaxial geogrid demonstrated significantly higher resistance than the biaxial geogrid. The interlocking between soil and geogrid-layer increases as the soil particles produce larger displacements and rotations near the geogrid-reinforced zone. The movement of soil particles near the triaxial geogrid-layer was greater than the movement of soil particles near the biaxial geogrid geogrid-layer. Makkar [7] describes the effect of 3-D geogrid-layer on the performance of a square footing resting on reinforced sand using Plaxis 3-D software. The effect of the 3-D geogrid-reinforced sand was compared with the planar geogrid-reinforced sand bed and the unreinforced sand. The 3-D geogrid-reinforced sand performed better than traditional planar geogrid-reinforced sand. Planar geogrids with an optimal layer's number improve the bearing capacity of the sand by 3.7 times compared to unreinforced soil and 6.3 times for 3-D geogrids. Albuja-Sanchez [8] conducted an experimental study to illustrate how the geogrid-layer arrangement affects the bearing capacity of square footing on granular soils. The geogrid-layers under the square footing are arranged in three different arrangements: uniform, trapezoidal, and inverted trapezoidal, with two types of geogrids, biaxial and multi-axial. The most effective configuration for both biaxial and multi-axial geogrids is the trapezoidal configuration; this configuration increases the load-bearing capacity of these two types of geogrids by 36% and 33%, respectively. Trapezoidal arrangement uses 7.0% less geogrid material than uniform arrangement. Baadiga [9] describes a large-scale experimental model to investigate the effect of biaxial and triaxial geogrid-layers on the mechanical response of pavement layers. The bearing capacity of reinforced subbase layer with the triaxial geogrid is 1.26 times that of the biaxial geogrid. Mir [10] investigates the load-settlement behavior of square footings on poorly graded medium sand. The sand soil is reinforced with two different aperture shape of geogrid-layers, uniaxial and biaxial. The optimal values for (u/B) and (b/B) are 0.4 and 5.0, respectively. The optimal values of (h/B) are 0.30 and 0.40 for the uniaxial and biaxial geogrid-aperture shapes, respectively.

In this study, a 3D numerical model was carried out to investigate the affecting of geogrid-aperture size on the bearing capacity ratio (BCR) of square footing on reinforced fine-sand beds and the horizontal stress ratios (HSR) mobilized in the transverse and longitudinal directions. In addition, the investigated parameters are first geogrid-layer depth (u/B), geogrid-layer width (b/B), vertical spacing between consecutive geogrid-layers (h/B) and geogrid-layers number (N). Five opening sizes of the geogrid-layer are used in the study; the ratios between the opening size length and width are 1.0, 1.50, 2.0, 3.0, and 4.0. The geogrid-aperture size is changed from biaxial to uniaxial; the opening sizes are 50 mm x 50 mm, 50 mm x 75 mm, 50 mm x 100 mm, 50 mm x 150 mm, and 50 mm x 200 mm, respectively.

2. NUMERICAL F.E.M. MODEL

The Abaqus 3-D model is used to investigate the effect of geogrid-aperture size on the bearing capacity of fine-sand. The dimensions of fine-sand domain are 20 m in height, 40 m in width, and 40 m length. The boundary conditions of the vertical sides of the model are constrained in the horizontal direction, while the base of the model is constrained in all directions. The top surface of the model is free, where the square footing is placed with dimensions of 2.0 m x 2.0 m. The square footing is subjected to a vertical displacement of 10% of the footing width at which the bearing capacity is defined. The fine-sand is described in the numerical model by an elasto-plastic material with a non-associated flow rule and using the modified Drucker-Prager model with a hardening curve. The hardening curve of the cap plasticity model is described by Park and Byrne [11]. The unit weight of

the fine-sand is 18 kN/m^3, the elastic modulus is 20 MPa, and the shear strength parameters (friction angle and cohesion) are 30° and zero, respectively. The properties of fine-sand are shown in Table (1). The geogrid-aperture sizes used in this study vary and are listed in Table (2). The width and thickness of the geogrid ribs in the longitudinal and transverse directions are 5.0 mm and 2.0 mm, respectively. The fine-sand soil mass is described by an 8-node linear brick, reduced integration and hourglass control (C3D8R), while the geogrid-layers are described by 4-node doubly curved general-purpose shell, finite membrane strains (S4R). To describe the full contact and interlocking between the geogrid-layers and fine-sand, the geogrid is modeled by embedded region constraints, where the host region is a fine-sand soil and the embedded region is the geogrid material with the capability to implement Abaqus/standard [12], [13]. Figure 1 shows the fine-sand dimensions, geogrid arrangement, finite element meshing and 3D model.

Table 1. Properties of fine-sand

Property	Symbol	Value
Unit weight, (kN/m^3)	γ	18.0
Poisson's ratio	υ	0.35
Young's modulus, MPa	E	20
Material cohesion, (kPa)	C	1.6e^{-3}
	d*	0.01
Friction angle, (°)	ϕ	30
	β*	50.19
Cap eccentricity	R	0.40
Init. cap yield surface pos.	––	0
Tran. surface radius	α	0.05
Flow stress ratio	k	1.0
Relative density	Dr	40%

* $d = \frac{18\,x\,C\,x\cos\phi}{3-\sin\phi}$, $\tan\beta = \frac{6\,x\sin\phi}{3-\sin\phi}$

Table 2. Properties of geogrid-layer

Geogrid properties	Value
Rib thickness, mm	2.0
Rib width, mm	5.0
Aperture size, mm	(50 x 50) – (50 x 75) – (50 x 100) – (50 x 150) – (50 x 200)
Axial stiffness, kN/m	1000
Ult. tensile strength (Tult)	50 kN/m
Poisson's ratio	0.35
Young's modulus, MPa	500
Unit weight, (kN/m^3)	10.0

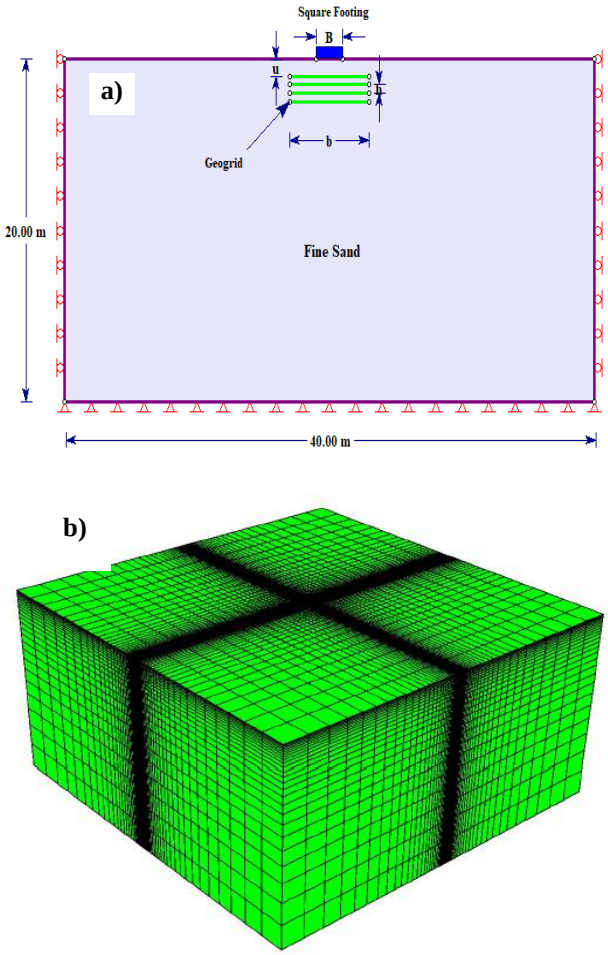

Figure 1: a) Numerical model dimensions and the geogrid arrangement, b) Finite element mesh and 3-D model

3. RESULTS AND DISCUSSION

A series of 3D numerical models were conducted on fine-sand with dimensions of 40m x 40m x 20m and supports of 2.0m x 2.0m square footing. Using a geogrid-layer as a reinforcing-layer enhances the bearing capacity of fine-sand and reducing the total settlement of the square footing. Bearing capacity ratio (BCR) is a dimensionless factor to describe the ratio between the bearing capacity of reinforced fine-sand and unreinforced sand, as described in Equation (1). The horizontal stresses transferred to the fine-sand in X and Y directions depend on the geogrid axial stiffness and the geogrid-aperture size. The horizontal stress ratio (HSR) is the ratio between the horizontal stresses of reinforced and unreinforced fine-sand, as described in equation (2).

$$BCR = q_{ur\ (reinforced)} / q_{u\ (unreinforced)} \quad (1)$$

$$HSR = HS_{\ (reinforced)} / HS_{\ (unreinforced)} \quad (2)$$

Where:

$q_{ur\ (reinforced)}$ = ultimate bearing capacity of reinforced soil.

$q_{u\ (unreinforced)}$ = ultimate bearing capacity of unreinforced soil

$HS_{\ (reinforced)}$ = Horizontal stress (X or Y) transmitted to the reinforced soil.

$HS_{\ (unreinforced)}$ = Horizontal stress (X or Y) transmitted to the unreinforced soil

3.1. Bearing Capacity of unreinforced Fine-sand

The bearing capacity of shallow foundations is calculated using bearing capacity theory, in which a failure mechanism is analyzed and expressed in terms of mobilized shear resistance and failure geometry. Bearing capacity failure in sandy soils occurs in three forms: general shear failure, local shear failure, and punching shear failure. General shear failure occurs in soils with relative density (D_r) greater than 70%; local shear failure occurs in soils with a relative density between 30 and 70%; and punching shear failure occurs in sand with a relative density of less than 30%. Meyerhof (1963) proposed a formula for calculating the ultimate bearing capacity (q_{ult}), which is similar to the formula proposed by Terzaghi, but introduced other coefficients such as shape factors, depth factors and inclination factors for the cases where the load line is inclined to the vertical, Equation (3) describes the bearing capacity equation assuming the general shear failure (Dr > 70%)[14].

$$q_{ult.} = c\ N_c\ S_c\ d_c\ i_c + q_o\ N_q\ S_q\ d_q\ i_q + 0.5\ \gamma\ B\ N_\gamma\ S_\gamma\ d_\gamma\ i_\gamma \quad (3)$$

Where:

N_c, N_q, N_γ: Meyerhof's bearing capacity factors depend on soil friction angle, ϕ.

S_c, S_q, S_γ: Shape factors

d_c, d_q, d_γ: Depth factors

i_c, i_q, i_γ: Incline load factors

q_o: Overburden pressure

For local shear failure (30% < Dr < 70%), the Meyerhof bearing capacity factors are reduced by a modified factor as suggested by Vesic (1975)[14]. The modified factor (k) depends on the relative density of sand as described in Equation (4) and (5).

$$\phi' = \tan^{-1}(k \times \tan\phi) \quad (4)$$

$$k = 0.67 + D_r - 0.75 \times (Dr^2) \quad (5)$$

For fine-sand with a relative density of 40%, a friction angle of 30° and a unit weight of 18.0 kN/m^3, the bearing capacity of unreinforced fine-sand supporting a square footing with a width of 2.0 m is 180.46 kPa, according to Meyerhof's Equation and Vesic's modification factor. Abaqus 3-D is used to simulate the numerical model of unreinforced fine-sand to verify the efficiency of the proposed model with Meyerhof equation. From the Abaqus results, the bearing capacity at a settlement of 10% footing width is defined using the stress-settlement curve. The bearing capacity determined from the Abaqus results is 165 kPa. The results showed good agreement with the results calculated using the Meyerhof equation, the Abaqus model is a good tool for estimating the bearing capacity of square footing on reinforced fine-sand. Figure (2) shows the settlement versus vertical stress of unreinforced fine-sand.

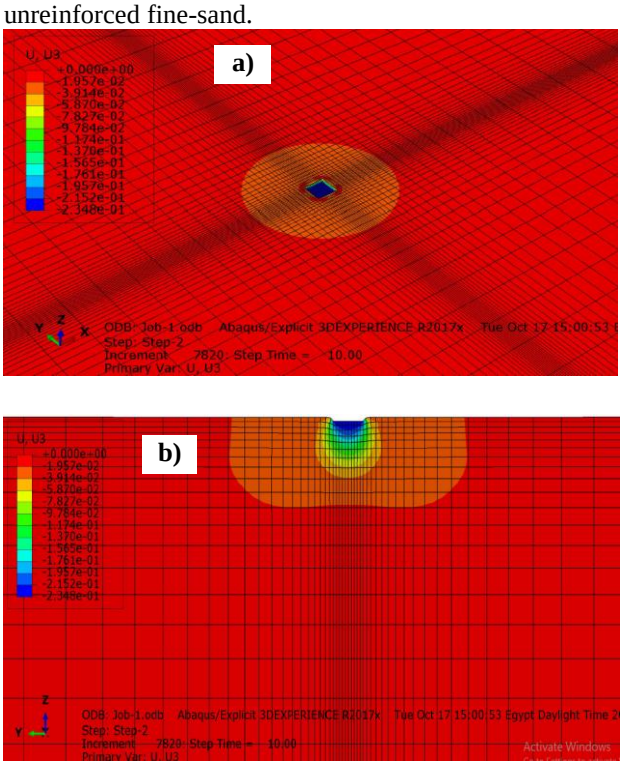

Figure 2: a) Settlement shading in 3-D, b) Cross section of settlement shading

3.2. Bearing Capacity of Reinforced Fine-sand

A wide range of parameters are considered in this study, such as first geogrid-layer depth, geogrid-layer width, vertical spacing between the successive geogrid-layers, and geogrid-layers number, to investigate the bearing capacity of reinforced fine-sand with geogrid-layer with different values of aperture size as shown in Figure (3). Figure (4) shows the settlement values for geogrid-aperture sizes of 50 mm x 50 mm and 50 mm x 200 mm. All studied parameters are listed in Table (3).

Table 3. Parametric Study and Geogrid Dimensions.

N	u/B	b/B	h/B	Geogrid-Aperture Size Ratio				
1	0.1	3	0	1.0	1.50	2.0	3.0	4.0
1	0.2	3	0	1.0	1.50	2.0	3.0	4.0
1	0.3	3	0	1.0	1.50	2.0	3.0	4.0
1	0.4	3	0	1.0	1.50	2.0	3.0	4.0
1	0.5	3	0	1.0	1.50	2.0	3.0	4.0
1	0.3	1	0	1.0	1.50	2.0	3.0	4.0
1	0.3	2	0	1.0	1.50	2.0	3.0	4.0
1	0.3	3	0	1.0	1.50	2.0	3.0	4.0
1	0.3	4	0	1.0	1.50	2.0	3.0	4.0

1	0.3	5	0	1.0	1.50	2.0	3.0	4.0
2	0.3	3	0.10	1.0	1.50	2.0	3.0	4.0
2	0.3	3	0.15	1.0	1.50	2.0	3.0	4.0
2	0.3	3	0.20	1.0	1.50	2.0	3.0	4.0
2	0.3	3	0.30	1.0	1.50	2.0	3.0	4.0
2	0.3	3	0.40	1.0	1.50	2.0	3.0	4.0
1	0.3	3	0	1.0	1.50	2.0	3.0	4.0
2	0.3	3	0.15	1.0	1.50	2.0	3.0	4.0
3	0.3	3	0.15	1.0	1.50	2.0	3.0	4.0
4	0.3	3	0.15	1.0	1.50	2.0	3.0	4.0
5	0.3	3	0.15	1.0	1.50	2.0	3.0	4.0

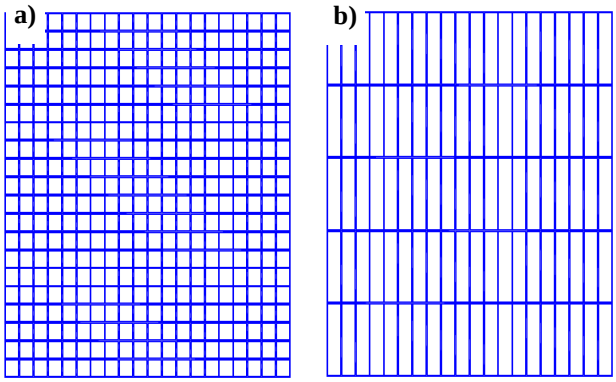

Figure 3: a) Geogrid size of 50 mmx 50 mm, b) Geogrid size of 50 mmx 200 mm

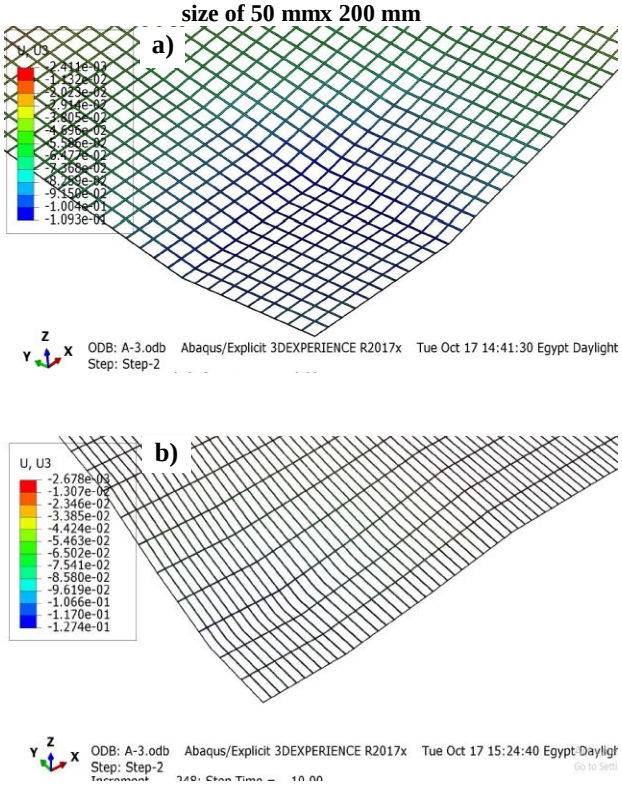

Figure 4: Settlement values a) geogrid size of 50 mm x 50 mm, b) geogrid size of 50 mm x 200 mm

3.2.1 First Geogrid-Layer Depth (u/B)

In the numerical model, a square footing is placed on surface of fine-sand and reinforced with a geogrid-layer with different aperture sizes to investigate the bearing capacity of the square footing with dimensions of 2.0 m x 2.0 m. The first geogrid-layer depth varies from (u/B) = 0.10 to (u/B) = 0.40 for each case of geogrid-aperture size. The geogrid-aperture sizes used in the study are 50 mm x 50 mm, 50 mm x 75 mm, 50 mm x 100 mm, 50 mm x 150 mm and 50 mm x 200 mm to achieve a ratio between the length and width of the geogrid opening $(L/B)_{geogrid}$ of 1.0, 1.50, 2.0, 3.0 and 4.0, respectively. For each case studied, the bearing capacity ratio (CBR) and the horizontal stresses transferred to the fine-sand in the X and Y directions are determined. The (BCR) values decreased with increasing $(L/B)_{geogrid}$, the optimal value of (BCR) is at $(L/B)_{geogrid}$ = 1.0 or biaxial geogrid, the (BCR) values increase with the (u/B) value up to (u/B) = 0.30 and then decrease with increasing (u/B) values. At (u/B) = 0.30, the BCR values are 3.73, 3.54, 3.41, 3.29 and 3.28 for a $(L/B)_{geogrid}$ of 1.0, 1.50, 2.0, 3.0 and 4.0, respectively. The (BCR) values decrease by 12.06% when the $(L/B)_{geogrid}$ is varied from 1.0 to 4.0.

HSR-(Cross) and HSR-(Machine) are defined as the ratio between the horizontal stresses transferred to the fine-sand using the geogrid-layer and the horizontal stress of the unreinforced fine-sand in X or (Cross) and Y or (Machine) directions. The HSR-(Cross) decreased with the increasing $(L/B)_{geogrid}$ for all cases of (u/B) values. For (u/B) = 0.30, the HSR-(Cross) values are 1.70, 1.64, 1.59, 1.56, and 1.46 for $(L/B)_{geogrid}$ values of 1.0, 1.50, 2.0, 3.0 and 4.0, respectively. HSR-(Cross) decreases by 14.11% when $(L/B)_{geogrid}$ varies between 1.0 and 4.0 as shown in Figure (5). At the optimal value of (u/B) = 0.30, HSR-(Machine) decreases with increasing $(L/B)_{geogrid}$; these values are 1.69, 1.61, 1.54, 1.48, and 1.41 for the $(L/B)_{geogrid}$ values of 1.0, 1.50, 2.0, 3.0, and 4.0, respectively. At (u/B) = 0.30, the HSR-(Machine) decreases by 16.56% when $(L/B)_{geogrid}$ varies between 1.0 and 4.0. The results show that the degree of interlocking between the soil and the geogrid-layer depends on the $(L/B)_{geogrid}$ and the (u/B). The most efficient values of $(L/B)_{geogrid}$ and (u/B) for increasing (BCR) and (HSR) are 1.0 and 0.30, respectively.

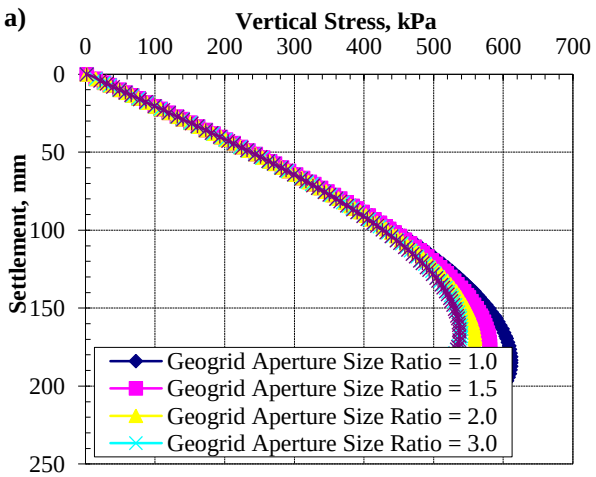

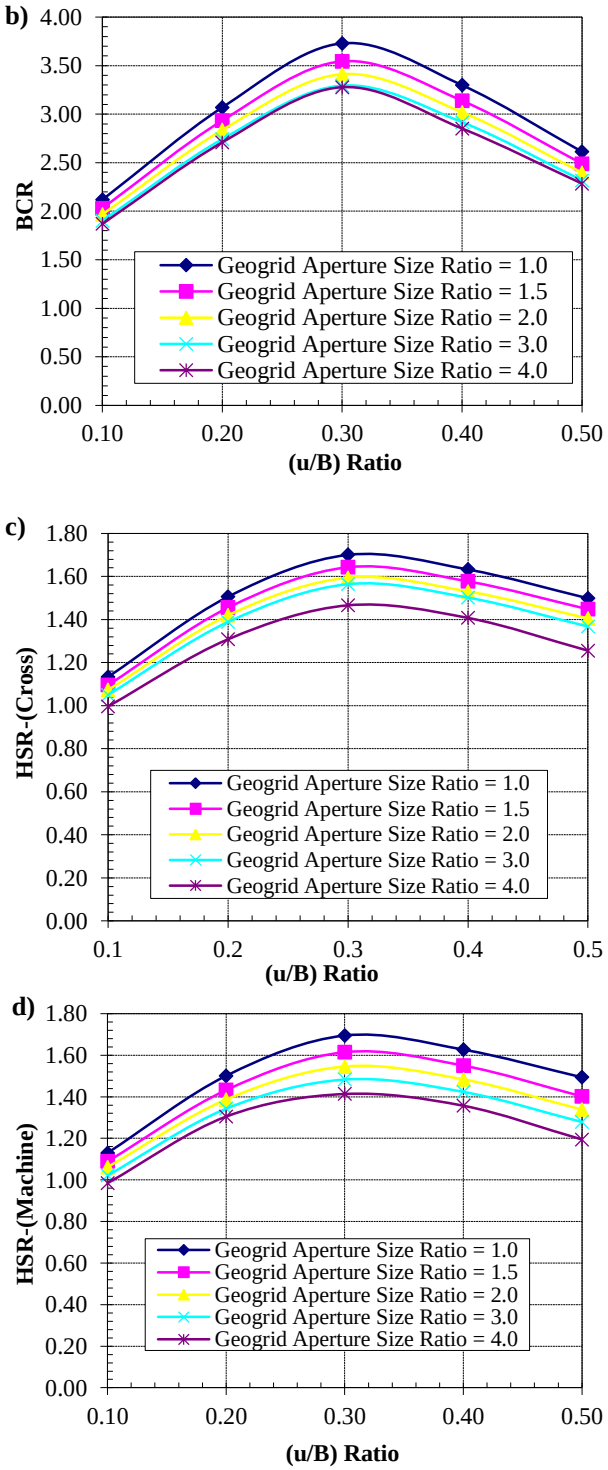

Figure 5: a) Settlement versus vertical stress for different values of geogrid-aperture size ratio at u/B = 0.30; b) BCR versus u/B ratio, c) HSR-(Cross) versus u/B ratio, d) HSR-(Machine) versus u/B ratio

3.2.2. Geogrid-Layer Width (b/B)

The geogrid-layer width under a square footing on reinforced fine-sand is investigated using Abaqus software. The geogrid-layer width ranges from B to 5.0 x B. The geogrid-aperture sizes are varied for each case of the (b/B) ratio, where the ratio of the geogrid opening size is 1.0, 1.5, 2.0, 3.0, and 4.0. Figure (6) shows the numerical results of the (BCR) values, HSR-(Cross) and HSR-(Machine). The (BCR) values increase with the (b/B) ratio until (b/B) = 3.0 and then decrease for all cases of $(L/B)_{geogrid}$. However, the (BCR) values decrease with increasing $(L/B)_{geogrid}$ ratio. The (BCR) values for the $(L/B)_{geogrid}$ = 1.0 are 3.16, 3.63, 3.73, 3.28, 3.25 with a variation of the (b/B) ratios of 1.0, 2.0, 3.0, 4.0 and 5.0, respectively. Furthermore, the (BCR) values of $(L/B)_{geogrid}$ ratio = 4.0 are 2.88, 3.12, 3.27, 2.92, 2.90 with a variation of (b/B) values of 1.0, 2.0, 3.0, 4.0 and 5.0, respectively. The values of horizontal stresses, HSR-(Cross), transferred to the reinforced fine-sand are 1.33, 1.621, 1.70, 1.67 and 1.60 for $(L/B)_{geogrid}$ = 1.0, while these values are 1.16, 1.39, 1.46, 1.42 and 1.33 for $(L/B)_{geogrid}$ = 4.0 when the (b/B) ratios are 1.0, 2.0, 3.0, 4.0 and 5.0, respectively. The values of horizontal stresses transferred to the reinforced fine-sand HSR-(Machine) are 1.33, 1.621, 1.70, 1.67 and 1.60 for $(L/B)_{geogrid}$ = 1.0, while these values are 1.12, 1.33, 1.40, 1.37 and 1.30 for $(L/B)_{geogrid}$ = 4.0 when the (b/B) ratios are 1.0, 2.0, 3.0, 4.0 and 5.0, respectively.

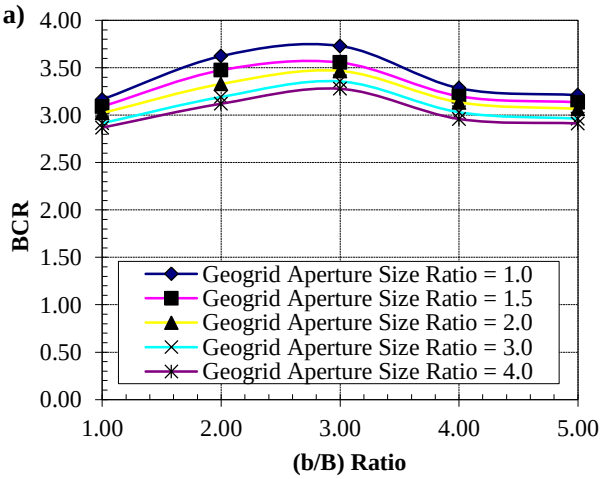

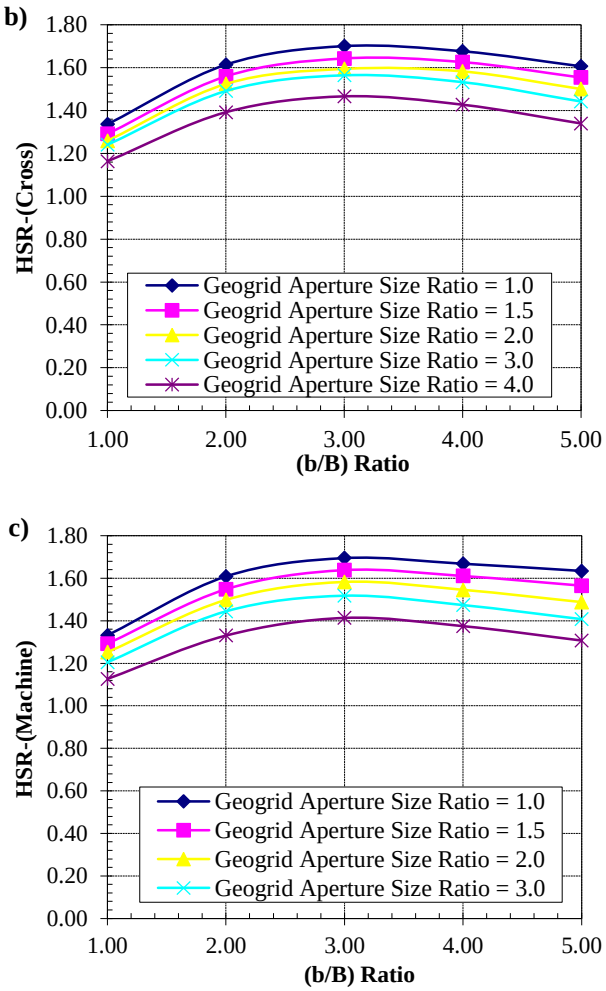

Figure 6: a) BCR versus b/B ratio, b) HSR-(Cross) versus b/B ratio, c) HSR-(Machine) versus b/B ratio for different values of geogrid-aperture size ratio

3.2.3. Vertical Spacing between Geogrid-Layers (h/B)

To study the effect of the vertical spacing between geogrid-layers on the (BCR) and (HSR) values transmitted to the fine-sand, the geogrid-layers width is 3.0 x B, the first geogrid-layer depth is 0.30 x B and the geogrid-layers number is 2.0 for a square footing of 2.0 m x 2.0 m. The vertical spacing between geogrid-layers used in this study is 0.10, 0.15, 0.20, 0.30, and 0.40 of the footing width. Figure (7) shows the effect of (h/B) for different cases of geogrid-aperture size ratios on the (BCR), HSR-(Cross) and HSR-(Machine) values. The (BCR) values decrease with increasing (h/B) ratio and geogrid-aperture size ratio. The (BCR) values are 4.80, 4.64, 4.51, 4.39 and 4.43 for the geogrid-aperture size ratios $(L/B)_{geogrid}$ of 1.0, 1.50, 2.0, 3.0 and 4.0 at (h/B) of 0.15. The (BCR) value decreased by 7.71% when the geogrid-aperture size ratio changed from 1.0 to 4.0. Furthermore, the HSR-(Cross) values are 2.36, 2.28, 2.21, 2.17 and 2.0 for the $(L/B)_{geogrid}$ values of 1.0, 1.50, 2.0, 3.0 and 4.0 at (h/B) of 0.15, while the HSR-(Machine) values are 2.36, 2.22, 2.11, 2.04 and 1.93 for the same $(L/B)_{geogrid}$ and (h/B) values.

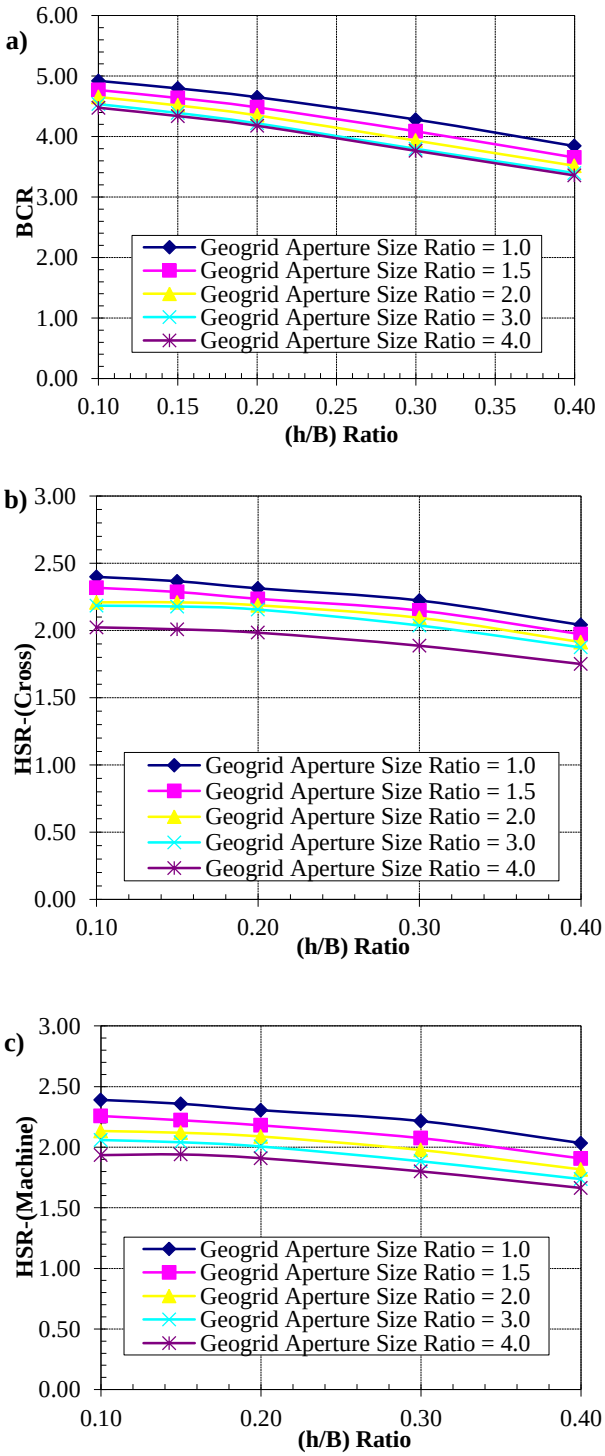

Figure 7: a) BCR versus h/B ratio, b) HSR-(Cross) versus h/B ratio, c) HSR-(Machine) versus h/B ratio for different values of geogrid-aperture size ratio

3.2.4. Geogrid-Layers Number (N)

Figure (8) shows the effect of geogrid-layers number on the (BCR) and (HSR) values transferred to the fine-sand in the X and Y directions. The numerical model is

carried out for the (u/B) value of 0.30, the (b/B) value of 3.0 and the (h/B) value of 0.15. The geogrid-layers number (N) varies between 1.0 and 5.0 and the $(L/B)_{geogrid}$ ratios are 1.0, 1.50, 2.0, 3.0, and 4.0. The (BCR) values increase with the geogrid-layers number (N) up to N = 3.0 and then the (BCR) values remain approximately constant. However, the (BCR) values decrease with increasing of $(L/B)_{geogrid}$ values. When a value of (N) is equal to 3.0, the (BCR) values are 5.02, 4.88, 4.77, 4.66 and 4.60 for $(L/B)_{geogrid}$ values of 1.0, 1.50, 2.0, 3.0 and 4.0, respectively. The (BCR) values decreased by 8.36% for the variation of $(L/B)_{geogrid}$ from 1.0 to 4.0.

The (HSR) values are transferred to the fine-sand in the cross direction or HSR-(Cross) increases with the geogrid-layers number (N), after (N) = 3.0 the HSR-(Cross) remains constant. The HSR-(Cross) values are 2.55, 2.47, 2.39, 2.33, and 2.18 for the $(L/B)_{geogrid}$ values of 1.0, 1.50, 2.0, 3.0 and 4.0, respectively. The HSR-(Cross) values decreased by 14.51% when the $(L/B)_{geogrid}$ values changed from 1.0 to 4.0. The HSR-(Machine) values are 2.55, 2.41, 2.31, 2.22 and 2.11 for the $(L/B)_{geogrid}$ values of 1.0, 1.50, 2.0, 3.0 and 4.0, respectively. The HSR-(Machine) decreased by 17.25% when the $(L/B)_{geogrid}$ values changed from 1.0 to 4.0. From the numerical results, it can be seen that the optimal value of the geogrid-layers number is 3.0. The biaxial geogrid-layer is considered the most efficient for the bearing capacity ratio and horizontal stress ratio in cross and machine directions.

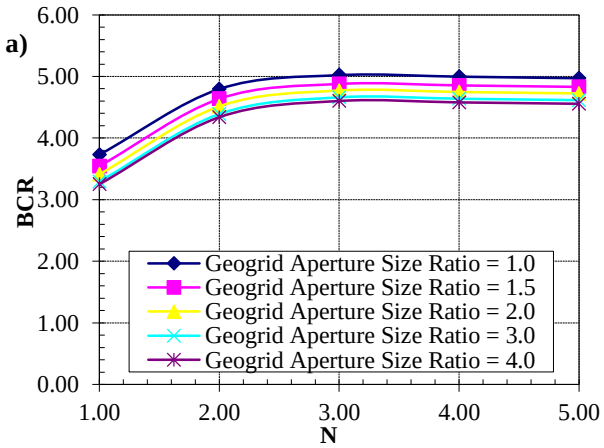

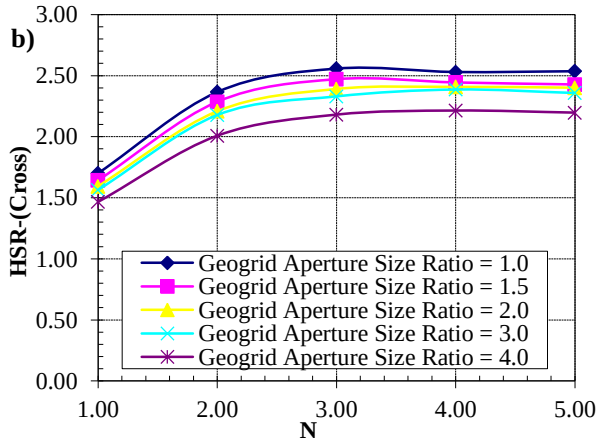

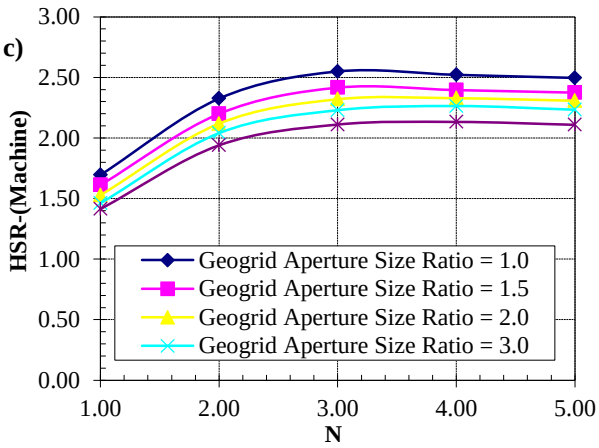

Figure 8: a) BCR versus N, b) HSR-(Cross) versus N, c) HSR-(Machine) versus N for different values of geogrid-aperture size ratio

In this research, the studied parameters are listed as (u/B), (b/B), (h/B), (N) and $(L/B)_{geogrid}$. The effect of these parameters on the (BCR), HSR-(Cross) and HSR-(Machine) values for the square footing is used to derive the relationship between them as described in Equations (6), (7) and (8). Figure (9) shows the correlation between the (BCR), HSR-(Cross), HSR-(Machine) values and the studied parameters.

$$(BCR)xN^2 = 2.24x\left[\frac{N}{\left(\frac{L}{B}\right)_{geogrid}+\left(\frac{u}{B}\right)+\left(\frac{b}{B}\right)+N+(2.1)^{\left(\frac{h}{B}\right)}}+N\right]^{2.44} \quad (6)$$

$$\text{HSR (CD)}xN^2 = 0.4897x\ln\left[\frac{N^2x\left(\frac{u}{B}\right)x\left(\frac{b}{B}\right)}{\left(\frac{L}{B}\right)_{geogrid}+N^2+(2.1)^{\left(\frac{h}{B}\right)}}\right]+2.5892 \quad (7)$$

$$\text{HSR (MD)}\ x\ N^2 = 0.4819\ x\ \ln\left[\frac{N^2x\left(\frac{u}{B}\right)x\left(\frac{b}{B}\right)}{\left(\frac{L}{B}\right)_{geogrid}+N^2+(2.1)^{\left(\frac{h}{B}\right)}}\right]+2.5327 \quad (8)$$

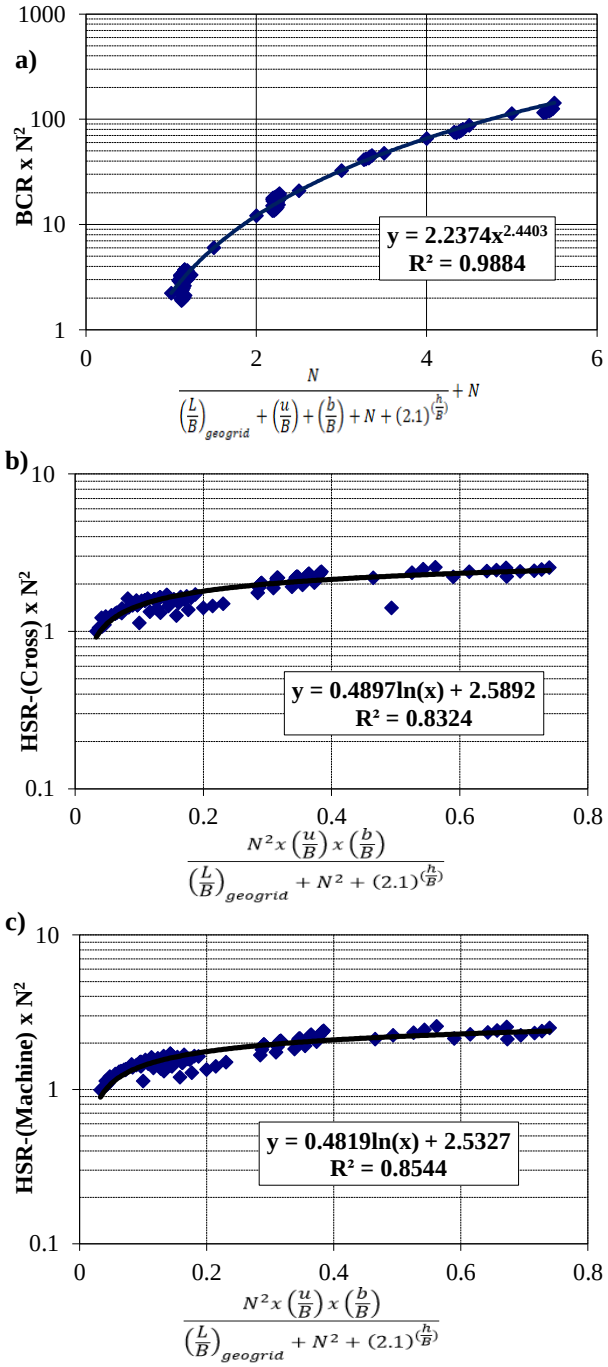

Figure 9: a) BCR versus studied parameters, b) HSR-(CD) versus studied parameters, c) HSR-(MD) versus studied parameters

4. CONCLUSIONS

In this study, 3-D models of square footings on geogrid-reinforced fine-sand are analyzed using the Abaqus (2017) software. The main objective of this research is to investigate the effects of geogrid-aperture size on the bearing capacity ratio (BCR) and the horizontal stresses (HS) transmitted to the fine-sand at the surface of the first geogrid-layer. The specified objectives are the effect of the first layer-layer depth (u/B), the geogrid-layers width (b/B), the vertical spacing between consequence geogrid-layers (h/B) and the geogrid-layers number (N). The effects of the studied parameters are discussed above and based on results of the 3-D model, the following conclusions can be drawn:

- The bearing capacity of the square footing on unreinforced sand from the Abaqus 3-D model is compared with that calculated from the Meyerhof equation (1963), the results illustrate that the difference between them does not exceed 8%. In addition, the Abaqus 3-D model used in this research is considered a good tool for determining the effects of the study parameters.
- In general, the bearing capacity of a square footing on geogrid-reinforced fine-sand is increased by using the proper dimensions and numbers of geogrid-layers, the horizontal stresses transferred to the fine-sand also increase. The results show that the interlocking between fine-sand and the geogrid-layers is enhanced due to the reduced movement of fine-sand particles.
- The bearing capacity ratio decreases with the increasing of geogrid-aperture size ratio. For the values of (u/B) = 0.3, (b/B) = 3.0, and N = 1.0, the maximum reduction in bearing capacity ratio is 12.06% when the geogrid-aperture size ratio increases from 1.0 to 4.0. The utilization of a biaxial geogrid-layer is more efficient than a uniaxial geogrid for the maximum BCR of square footing on geogrid-reinforced fine-sand.
- The maximum decrease in horizontal stress ratio in the cross direction is 14.51%, while that for horizontal stress in the machine direction is 17.25% when the geogrid-aperture size ratio increases from 1.0 to 4.0.
- The maximum value of the bearing capacity ratio of the reinforced fine-sand was achieved when the value (u/B) = 0.30 for all values of the geogrid-aperture size.
- The optimal value of the (b/B) ratio of the geogrid-layer under the square footing is 3.0 for all values of the geogrid-aperture size.
- The optimal vertical spacing (h/B) between each successive geogrid-layer is about 0.15 x B for all values of the geogrid-aperture size.
- The numerical results illustrate that the optimal number of geogrid-layers is 3.0 for all values of the geogrid-aperture size.

STATEMENTS AND DECLARATIONS

Competing interests: The authors declare that they have no known competing financial interests or personal relationships that could have appeared to influence the work reported in this paper.

Funding**:** This manuscript has no funding

5. REFERENCES

[1] J. P. Giroud and J. Han, "Design Method for Geogrid-Reinforced Unpaved Roads. II. Calibration and Applications," *J. Geotech. Geoenvironmental Eng.*, vol. 130, no. 8, pp. 787–797, 2004, doi: 10.1061/(asce)1090-0241(2004)130:8(787).

[2] A. Shafi and A. Minhas, "Modelling of Square Footing to Study the Enhancement of Load Carrying Capacity of Sand Using Geogrids," *J. Emerg. Technol. Innov. Res.*, vol. 6, no. 6, pp. 779–783, 2019.

[3] B. Durga Prasad, C. Hariprasad, and B. Umashankar, "Load-Settlement Response of Square Footing on Geogrid Reinforced Layered Granular Beds," *Int. J. Geosynth. Gr. Eng.*, vol. 2, no. 4, pp. 1–10, 2016, doi: 10.1007/s40891-016-0070-6.

[4] M. S. Ahmadi and P. N. Moghadam, "Effect of Geogrid Aperture Size and Soil Particle Size on Geogrid-Soil Interaction under Pull-Out Loading," *J. Text. Polym.*, vol. 5, no. 1, pp. 25–30, 2017.

[5] S. K. Das and N. K. Samadhiya, "A numerical parametric study on the efficiency of prestressed geogrid reinforced soil," in *E3S Web of Conferences*, 2020, pp. 1–7. doi: 10.1051/e3sconf/202020512004.

[6] J. Fu, J. Li, C. Chen, and R. Rui, "DEM-FDM coupled numerical study on the reinforcement of biaxial and triaxial geogrid using pullout test," *Appl. Sci.*, vol. 11, no. 19, 2021, doi: 10.3390/app11199001.

[7] F. M. Makkar and M. V Sreya, "Numerical Modelling of the Behaviour of 3D Geogrid Reinforced Soil Foundation," *J. Emerg. Technol. Innov. Res.*, vol. 9, no. 6, pp. 67–73, 2022.

[8] J. Albuja-Sánchez, L. Cóndor, K. Oñate, S. Ruiz, and D. Lal, "Influence of geogrid arrangement on the bearing capacity of a granular soil on physical models and its comparison to theoretical equations," *SN Appl. Sci.*, vol. 5, no. 9, 2023, doi: 10.1007/s42452-023-05474-w.

[9] R. Baadiga and U. Balunaini, "Evaluation of pavement design input parameters of biaxial and triaxial geogrid stabilized flexible pavements overlying soft subgrades," *Clean. Mater.*, vol. 9, no. December 2022, p. 100192, 2023, doi: 10.1016/j.clema.2023.100192.

[10] B. A. Mir and S. Ashraf, "Evaluation of Load-Settlement Behaviour of Square Model Footings Resting on Geogrid Reinforced Granular Soils," *2nd GeoMEast Int. Congr. Exhib. Sustain. Civ. Infrastructures*, no. November, 2018, doi: /doi.org/10.1007/978-3-030-01923-5_9.

[11] S. S. Park and P. M. Byrne, "Stress densification and its evaluation," *Can. Geotech. J.*, vol. 41, no. 1, pp. 181–186, 2004, doi: 10.1139/t03-076.

[12] C. A. E. User, "Abaqus theory manual," *Abaqus 6.13 Doc.*, no. Dassault Systemes Simulia Corp., Providence, RI, USA., 2014.

[13] S. Helwany, *Applied Soil Mechanics with Abaqus Applications*. 2007.

[14] Braja M. Das, *Shallow Foundation Bearing Capacity and Settlement*, Second. New York, 2009.